Heliyon 10 (2024) e38822

Contents lists available at ScienceDirect

Heliyon

journal homepage: www.cell.com/heliyon

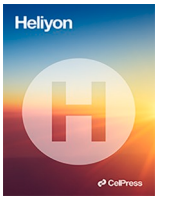

Research article

SHANK2-AS3: A potential biomarker for Parkinson's disease and its role in neuronal apoptosis via NF-κB signaling in SH-SY5Y cells

Qiong Huang [a,b,1], Dani Qin [c,1], Chunyan Chen [b,1], Yu Kang [a], Haocong Chen [a], Min Xu [b,**], Rao Fu [b,***], Xiaohua Dong [a,*]

[a] Hongqiao International Institute of Medicine, Tongren Hospital, Shanghai Jiao Tong University School of Medicine, Shanghai, China
[b] Department of Neurology, Tongren Hospital, Shanghai Jiao Tong University School of Medicine, Shanghai, China
[c] Department of Pediatrics, Yixing People's Hospital, No.75 Tongzhenguan Road, Yixing, Jiangsu, 214200, China

ARTICLE INFO

Keywords:
SHANK2-AS3
Cell apoptosis
Parkinson's disease

ABSTRACT

Parkinson's disease (PD) is a progressive neurodegenerative disorder primarily driven by the degeneration of dopaminergic neurons, manifesting as hallmark symptoms such as muscle rigidity, tremors, and motor dysfunction, all of which severely compromise patients' quality of life. Increasing evidence highlights the critical role of long non-coding RNAs (lncRNAs) in PD pathogenesis. However, the specific involvement of SHANK2-AS3 in PD remains unclear. By reanalyzing the dysregulated lncRNAs from the GSE22491 dataset, we identified a significant upregulation of SHANK2-AS3 in PD patients compared to healthy controls. This finding was further validated in a new cohort of PD patients, where SHANK2-AS3 expression was notably elevated in peripheral blood samples. Additionally, we observed a marked increase in SHANK2-AS3 expression in MPTP-treated SH-SY5Y cells, a commonly used *in vitro* PD model. Functional assays demonstrated that SHANK2-AS3 knockdown attenuated MPTP-induced apoptosis, reduced reactive oxygen species (ROS) accumulation, and improved mitochondrial function. In contrast, SHANK2-AS3 overexpression exacerbated neuronal apoptosis. RNA sequencing and Western blot analyses revealed that the NF-κB signaling pathway is involved in SHANK2-AS3-mediated neuronal apoptosis. In summary, our findings suggest that SHANK2-AS3 plays a critical role in PD pathogenesis and represents a potential therapeutic target for mitigating neuronal damage in PD.

1. Introduction

Parkinson's disease (PD) is a neurodegenerative disorder characterized by the progressive loss of dopaminergic neurons in the substantia nigra of the brain [1]. With the aging population contributing to its rising prevalence, it has been reported that the global crude prevalence of PD increased by approximately 74 % between 1990 and 2016 [2]. Clinically, PD manifests with hallmark motor symptoms, including tremors, rigidity, bradykinesia, and postural instability [3]. In addition to motor impairments, PD also presents

* Corresponding author.
** Corresponding author.
*** Corresponding author.
E-mail addresses: 13601664630@163.com (M. Xu), furaocmu@163.com (R. Fu), njfishxiaohua@163.com (X. Dong).
[1] These authors contribute equally to this work.

https://doi.org/10.1016/j.heliyon.2024.e38822
Received 20 June 2024; Received in revised form 12 September 2024; Accepted 30 September 2024
Available online 1 October 2024

non-motor symptoms, such as cognitive decline, sleep disturbances, hyposmia, and autonomic dysfunction, all of which significantly reduce patients' quality of life [4]. The exact etiology of PD remains elusive, though it is thought to result from a complex interplay of genetic, environmental, and lifestyle factors [5]. Current treatments for PD are primarily symptomatic, with L-DOPA being the cornerstone of therapy, often combined with other agents like MAO-B inhibitors and COMT inhibitors [6]. However, no curative treatment exists. As the disease progresses, patients frequently develop symptoms that are resistant to treatment and experience adverse effects from long-term medication use. This highlights the pressing need to further elucidate PD pathophysiology and develop more effective therapies.

Accumulating evidence indicates that cell death play a significant role in the pathology of PD [7]. Apoptosis, or programmed cell death, is central to PD's pathogenesis. In PD, dopaminergic neurons in the substantia nigra undergo apoptosis, resulting in the characteristic motor symptoms of the disease. Several biological processes and signaling pathways are involved in neuronal apoptosis in PD. Notably, mitochondrial dysfunction drives energy deficits, oxidative stress, and neuronal death, contributing to disease progression [8]. Additionally, NF-κB signaling is crucial in mediating oxidative stress, its activation promotes the expression of pro-inflammatory cytokines and exacerbates neuronal apoptosis, further advancing neurodegeneration and disease progression [9]. Apoptotic pathways mediated by mitochondrial dysfunction, cytochrome *c* release, and caspase activation lead to cell death. Furthermore, dysregulation of anti-apoptotic proteins, such as Bcl-2 family members, and pro-apoptotic factors like Bax, contributes to neuronal apoptosis in PD [10]. Understanding these mechanisms of neuronal apoptosis is essential for developing therapeutic strategies aimed at preventing or slowing neurodegeneration.

Long non-coding RNAs (lncRNAs) are RNA molecules longer than 200 nucleotides that do not encode proteins. In recent years, research has shown that lncRNAs are abundantly expressed in brain tissue and play critical roles in neurodegenerative diseases [11,12]. In Parkinson's disease (PD), lncRNAs are key regulators of gene expression, cell signaling, neuronal function, and survival. For instance, lncRNA HOTAIR modulates the expression of the SNCA (α-synuclein) gene by regulating miR-126-5p, thereby influencing the development and progression of PD [13]. Additionally, lncRNA NEAT1 has been implicated in the regulation of α-synuclein in PD [14,15]. However, whether other lncRNA participate in the pathogenesis of PD is still poorly understood.

In this study, we identified SHANK2-AS3 as a dysregulated lncRNA in Parkinson's disease (PD) through an analysis of the GSE22491 dataset [16]. Clinical samples further validated the upregulation of SHANK2-AS3 in PD patients. Using an *in vitro* PD model, SH-SY5Y cells treated with 1-Methyl-4-phenyl-1,2,3,6-tetrahydropyridine (MPTP), we observed a significant increase in SHANK2-AS3 expression. Knockdown of SHANK2-AS3 alleviated MPTP-induced apoptosis in SH-SY5Y cells, whereas its overexpression exacerbated neuronal damage. Mechanistically, RNA sequencing and Western blot analysis revealed the potential involvement of the NF-κB signaling pathway in SHANK2-AS3-mediated neuronal injury. These findings suggest that SHANK2-AS3 could serve as a promising therapeutic target for the treatment of PD.

2. Material and methods

2.1. Sample collection

The peripheral blood samples were collected from Shanghai Tongren Hospital, including samples from Parkinson's disease (PD) patients and healthy older individuals. For PD samples, inclusion criteria involved the presence of bradykinesia (slow movement) along with at least one of the following: resting tremor, rigidity, or postural instability. Exclusion criteria comprised patients with secondary parkinsonism due to known causes such as drug-induced parkinsonism, vascular parkinsonism, or other neurodegenerative disorders. All patients met the clinical diagnostic criteria for Parkinson's Disease set by the Movement Disorder Society (MDS) [17]. Control samples were collected from healthy elderly individuals with no underlying diseases or history of medication usage. A total of 31 samples were collected, consisting of 11 healthy controls and 20 PD patients. Clinical information for both PD and control samples is detailed in Table 1. Written informed consent was obtained from all participants, and the sample collection protocol was approved by the ethical committee of Shanghai Tongren Hospital (2018-030-01).

2.2. Bioinformatics data

LncRNA expression profiles of Parkinson's disease (PD) patients were retrieved from Gene Expression Omnibus (GEO) at https://www.ncbi.nlm.nih.gov/geo/. Specifically, the GEO Datasets GSE22491 were downloaded and utilized directly for subsequent analysis.

Table 1
Baseline characteristics of PD patients and control subjects.

Characteristics	PD	Control
Number	20	11
Age (mean ± SD, range)	71.4 ± 8.52 (52–83)	73.81 ± 6.49 (65–87)
Sex		
Male, n (%)	9 (45 %)	6 (54.5 %)
Female, n (%)	11 (55 %)	5 (45.4 %)
Hoehn-Yahr	2.15 ± 0.74 (1–3)	–
Treated	20 (100 %)	–

2.3. Cell culture and treatment

SH-SY5Y were cultured in Ham's F-12 K (Kaighn's) medium (Gibco) with 15 % fetal bovine serum (Gibco), 1 % penicillin and 1 % streptomycin (Gibco), maintained at 37 °C with 5 % CO2 in cell incubator. MPTP were purchased from MedChamExpress company (MCE, HY-15608). MPTP at different concentration (2 mM, 4 mM, and 8 mM) was added to the medium and incubated for 24 h.

SH-SY5Y cells were cultured in Ham's F-12 K (Kaighn's) medium (Gibco) supplemented with 15 % fetal bovine serum (Gibco), 1 % streptomycin, and 1 % penicillin (Gibco). The cells were maintained at 37 °C with 5 % CO2 in the cell incubator. MPTP (MPTP hydrochloride) was purchased from MedChamExpress company (MCE, HY-15608). Different concentrations of MPTP (2 mM, 4 mM, and 8 mM) were added to the cell culture medium and incubated for 24 h. The NF-kB signaling inhibitor PDTC (Pyrrolidinedithiocarbamic acid; Beyotime Biotechnology, S1808, Shanghai, China) was used to treat SH-SY5Y cells at a concentration of 50 μM.

2.4. Overexpression or knockdown of SHANK-AS3 in SH-SY5Y

For overexpression of SHANK-AS3 in SH-SY5Y, the lentivirus containing the full length of SHANK-AS3 were used. The vector of pLV4ltr-Puro-CMV was used for package the SHANK-AS3 overexpression lentivirus. For knockdown of SHANK-AS3 in SH-SY5Y, the lentiviruses containing interfering sequences targeting SHANK-AS3 were utilized for knocking down SHANK-AS3 expression. The target sequences of SHANK-AS3 used were as follows: si1: GTGAGAGAATGTTTCTGATAA, si2: GAAGAAACCGAGTGAGGATGA, si3: GCCCATCATTTGGAAAGGGAA. The vector of pLV3ltr-ZsGreen-Puro-U6 was used for package the SHANK-AS3 knockdown lentivirus. The procedures for SHANK2-AS3 knockdown or overexpression were conducted as follows: when SH-SY5Y cells reached 40%–60 % confluence, lentivirus with SHANK2-AS3 knockdown or overexpression, along with 10 μg/mL Polybrene, were added to the fresh culture medium. The cells were then incubated for 24 h for lentivirus transfection. Subsequently, the medium was replaced, and the cells were cultured for an additional 48 h for further experimentation.

2.5. RT-qPCR

The peripheral blood samples were collected using BD PAXgene Blood RNA Tubes (BD, #762165). Total RNA was extracted from the peripheral blood samples using the PAXgene Blood RNA Kit (QIAGEN, #762174) following the manufacturer's instructions. cDNA was synthesized using the HiScript II 1st Strand cDNA Synthesis Kit (Vazyme, China) according to the kit's protocol. For quantitative PCR (qPCR), the primer sequences used for SHANK2-AS3 were ACCTGAGCTGATGGCACAAC (Forward) and CCCCACAGAATCCGTGTCTT (Reverse). The primer sequences for 18s RNA were GCGCCGCTAGAGGTGAAATTC (Forward) and TTGGCAAATGCTTTCGCTC (Reverse).

2.6. CCK8 assay

Cell Counting Kit-8 (CCK8, Beyotime, China) were used to detect the cell viability. Briefly, the reaction solution was added to the culture medium at a dilution of 1/10. Subsequently, the cells were incubated for 1–2 h at the cell incubator. The absorbance was then measured at 450 nm.

2.7. Calcein-PI staining

Cell activity and cytotoxicity were assessed using the Calcein/PI Cell Viability/Cytotoxicity Assay Kit (Beyotime, China) following the manufacturer's protocol. After washing the cells once with PBS, the Calcein/PI working solution (1 ×) was added. The cells were then incubated for 30 min at the cell incubator. Live and dead cells were distinguished using an Inverted fluorescence microscope (Nikon, TS2-S-SM, Japan), with red indicating dead cells and green indicating live cells.

2.8. Western blot

The Western blot was performed as we previously reported [18]. Briefly, SH-SY5Y cells were lysed using RIPA (Radio Immunoprecipitation Assay) lysis buffer (P0013B, Beyotime, China) supplemented with 1 mM PMSF (Phenylmethanesulfonyl fluoride) (ST506, Beyotime, China). Protein separation was performed on 8%–20 % acrylamide/bisacrylamide gels, followed by transfer to PVDF membranes (Millipore, Billerica, USA). Unspecific protein binding was blocked using 5 % blocking reagent (1 × TBST containing 5 % defatted milk powder) for 1 h at room temperature. Primary antibodies were incubated with the membranes overnight at 4 °C in blocking reagent. After washing with 1 × TBST three times, membranes were incubated with HRP (horseradish peroxidase)-conjugated secondary antibodies in blocking reagent for 1 h at room temperature. Protein expression was detected using Tanon 6200 (Tanon, Shanghai, China). The primary antibody of Bcl-2 (#26593-1-AP, Proteintech), Bax (#50599-2-Ig, Proteintech), Caspase-3 (#9662, Cell Signaling Technology), Cleaved Caspase-3 (Asp175) (#9661, Cell Signaling Technology), NF-κB p65 (#8242S, Cell Signaling Technology), Phospho-NF-κB p65 (#3033S, Cell Signaling Technology), p-IKBα (#AF2002, Affinity), IKBα (#,AF5002, Affinity), β-Actin (#66009–1-Ig, Proteintech) were used for Western blot. And the secondary antibody of HRP-conjugated Affinipure Goat Anti-Mouse IgG (H + L) (#SA00001–1, Proteintech)/Anti-Rabbit IgG (H + L) (#SA00001–2, Proteintech) were used for Western blot.

2.9. Reactive oxygen species (ROS) and mitochondrial membrane potential (MMP) detection

The ROS assay and MMP assay were detected in living SH-SY5Y. The ROS assay kit (Applygene Technologies Inc., China) and the Mitro Tracker (Invitrogen, M7512, USA) were used for ROS and MMP detection, respectively. In brief, the cultured cell medium was aspirated, and 10 μM DHE and 200 nM MitroTracker Red probes were used to detect ROS and MMP levels in SH-SY5Y cells, respectively. The fluorescence intensity of ROS and MMP was immediately captured using a confocal microscope (Leica, SP8, Germany). ImageJ software was utilized to quantify the fluorescence intensity of ROS and MMP.

2.10. Immunofluorescence (IF)

The immunostaining was conducted as we previously reported [19]. SH-SY5Y cells were fixed with 4 % paraformaldehyde (PFA) for 20 min at 4 °C. Next, the cells were incubated with primary antibody against Phospho-NF-κB p65 (#3033S, Cell Signaling Technology) and then treated with secondary antibodies (Proteintech, SA00013-2). Confocal microscopy (Leica, SP8, Germany) was used to capture the images.

2.11. RNA-seq analysis

Total RNA was isolated using the RNA-easy Isolation Reagent (R701–01, Vazyme, Nanjing) following the manufacturer's

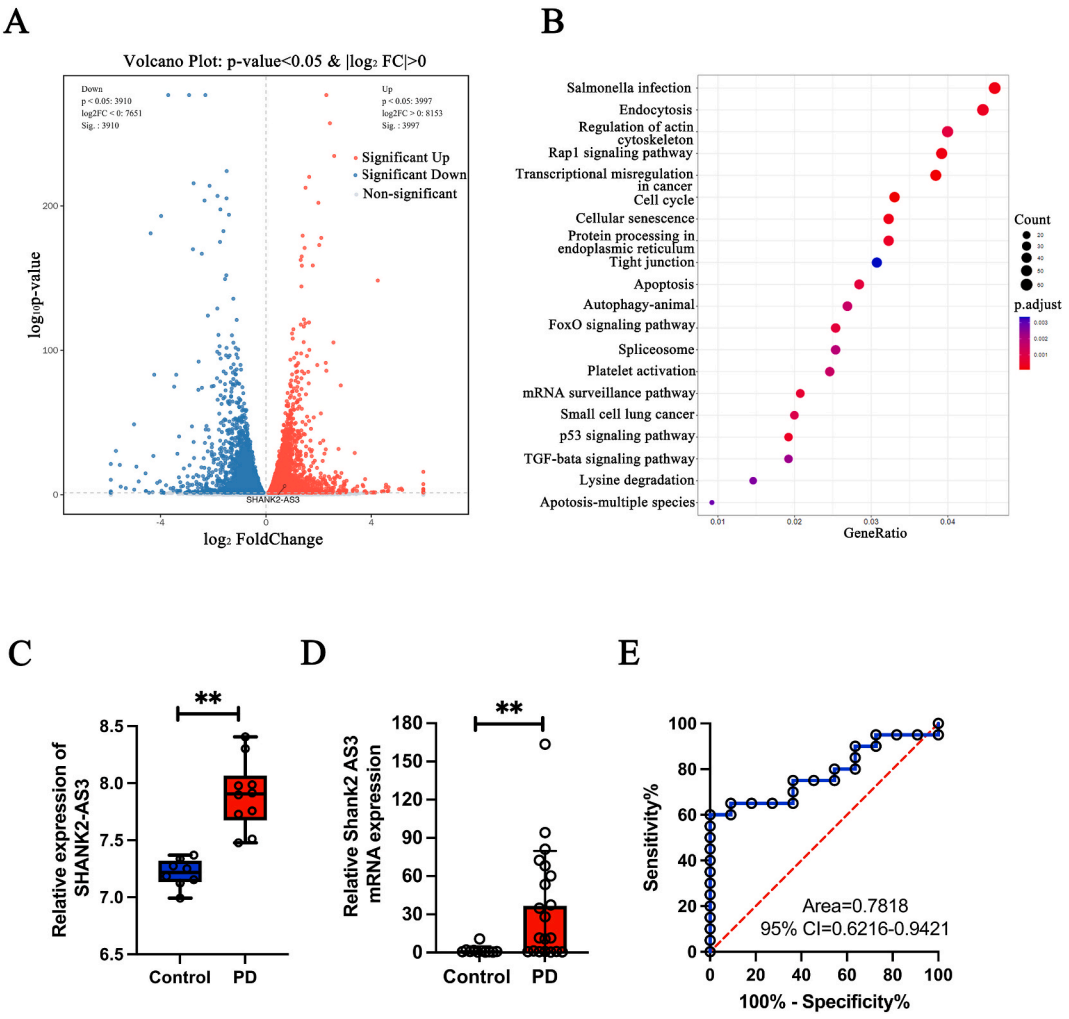

Fig. 1. Reanalysis of Differentially Expressed lncRNAs in PD Patients and Healthy Controls. (A) Volcano plot illustrating differentially expressed genes in PD patients compared to healthy controls. (B) KEGG enrichment analysis of dysregulated of lncRNAs in PD patients relative to controls. (C) Relative expression levels of SHANK2-AS3 in peripheral blood of PD patients versus elderly healthy controls. (D) Validated the expression of SHANK2-AS3 in the PD patients compared with healthy controls. (E) ROC curves demonstrating the diagnostic utility of SHANK2-AS3 levels in distinguishing PD patients from elderly individuals. Data represented as mean ± SD; $^{**}p < 0.01$.

guidelines. The RNA's purity and quantity were assessed using the NanoDrop 2000 spectrophotometer (Thermo Scientific, USA). Libraries were prepared using the TruSeq Stranded mRNA LT Sample Prep Kit (Illumina, San Diego, CA, USA) as per the manufacturer's instructions. Subsequent RNA-seq analysis was conducted by OE Biotech Co., Ltd. (Shanghai, China).

2.12. RNA sequencing and differentially expressed genes analysis

Illumina NovaSeq 6000 platform was used to sequenced. DESeq2 was employed for differential expression analysis, with significance set at $p < 0.05$ and $|\log2FC| > 1$ for identifying significantly differentially expressed genes (DEGs). Hierarchical cluster analysis using R (version 3.2.0) was conducted to visualize gene expression patterns across different groups and samples. A radar map displaying the expression of the top 30 genes, whether up-regulated or down-regulated DEGs, was generated using the R package ggradar. Enrichment analysis of DEGs was performed for GO, KEGG pathways, Reactome, and WikiPathways based on the hypergeometric distribution using R (version 3.2.0). Significant enrichment terms were identified and visualized using R (version 3.2.0) to create column diagrams, chord diagrams, and bubble diagrams illustrating the enriched terms.

2.13. Statistical analysis

Statistical analyses were performed by GraphPad Prism (Version 9.0.0). $p < 0.05$ was statistically significant. Error bar indicate SD.

3. Results

3.1. SHANK2-AS3 dysregulated in PD patients

To identify functional lncRNAs involved in the pathophysiological mechanisms of PD, we reanalyzed differentially expressed lncRNAs in the GEO database using GSE22491. Our analysis revealed 7907 differentially expressed mRNAs ($p < 0.05$, $|\log_2FC| > 0$) in the PBMCs of PD patients compared to controls (Fig. 1A). KEGG analysis suggested that the dysregulated lncRNA involved in the multiple cell progress, which including the cell apoptosis, cell autophagy and so on (Fig. 1B). Notably, SHANK2-AS3 was found to be upregulated in PD patients based on RNA-Seq analysis (Fig. 1C). To validate this finding, we extracted total RNA from the peripheral blood of an independent cohort of 20 PD patients and 11 age-matched healthy controls. qPCR results confirmed that SHANK2-AS3 expression was significantly higher in PD patients than in controls (Fig. 1D). Furthermore, the area under the curve (AUC) for SHANK2-AS3 in distinguishing PD patients from healthy controls was 0.78 (95 % CI, 0.6216–0.9421, $p < 0.05$, Fig. 1E), indicating that

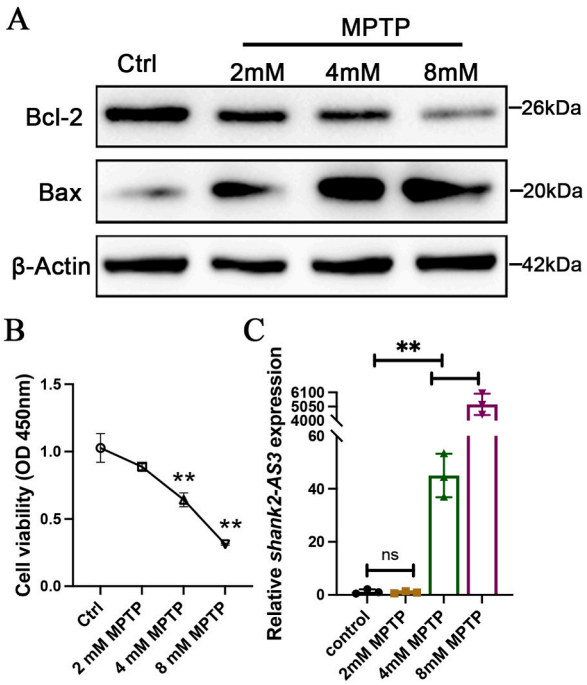

Fig. 2. SHANK2-AS3 Expression in MPTP-Induced SH-SY5Y Cells. (A) Western blot analysis of the expression levels of Bcl-2 and Bax in SH-SY5Y cells treated with 1 mM, 2 mM, and 4 mM MPTP for 24 h, compared to untreated controls. (B) Cell viability of SH-SY5Y cells following MPTP treatment, assessed using the CCK-8 assay, relative to control cells. (C) Relative expression of SHANK2-AS3 in SH-SY5Y cells treated with 1 mM, 2 mM, or 4 mM MPTP. Data represented as mean ± SD; $^{**}p < 0.01$; ns, no significance.

SHANK2-AS3 may play a significant role in PD pathogenesis.

3.2. SHANK2-AS3 upregulated in MPTP-treated SH-SY5Y

To investigate the role of SHANK2-AS3 in the pathogenesis of Parkinson's disease (PD), we employed an *in vitro* model of neuronal injury using SH-SY5Y cells treated with MPTP. SH-SY5Y cells were exposed to increasing concentrations of MPTP (2 mM, 4 mM, and 8 mM) for 24 h. MPTP treatment resulted in a significant downregulation of Bcl-2 expression and upregulation of Bax expression, indicating the induction of apoptosis (Fig. 2A). Moreover, CCK-8 assays showed a marked decrease in SH-SY5Y cell viability, with viability reduced to 0.64 ± 0.046 and 0.31 ± 0.006 following treatment with 4 mM and 8 mM MPTP, respectively (Fig. 2B). Importantly, SHANK2-AS3 expression was significantly upregulated in SH-SY5Y cells treated with 4 mM and 8 mM MPTP compared to control cells (Fig. 2C). These results confirm that the MPTP-induced SH-SY5Y cell model was successfully established at 4 mM and 8 mM MPTP concentrations, and the observed upregulation of SHANK2-AS3 suggests its potential role as a key regulator in PD pathogenesis.

3.3. SHANK2-AS3 knockdown mitigates MPTP-induced apoptosis in neuronal cells

To further elucidate the role of SHANK2-AS3 in MPTP-induced neuronal apoptosis, we knocked down SHANK2-AS3 expression

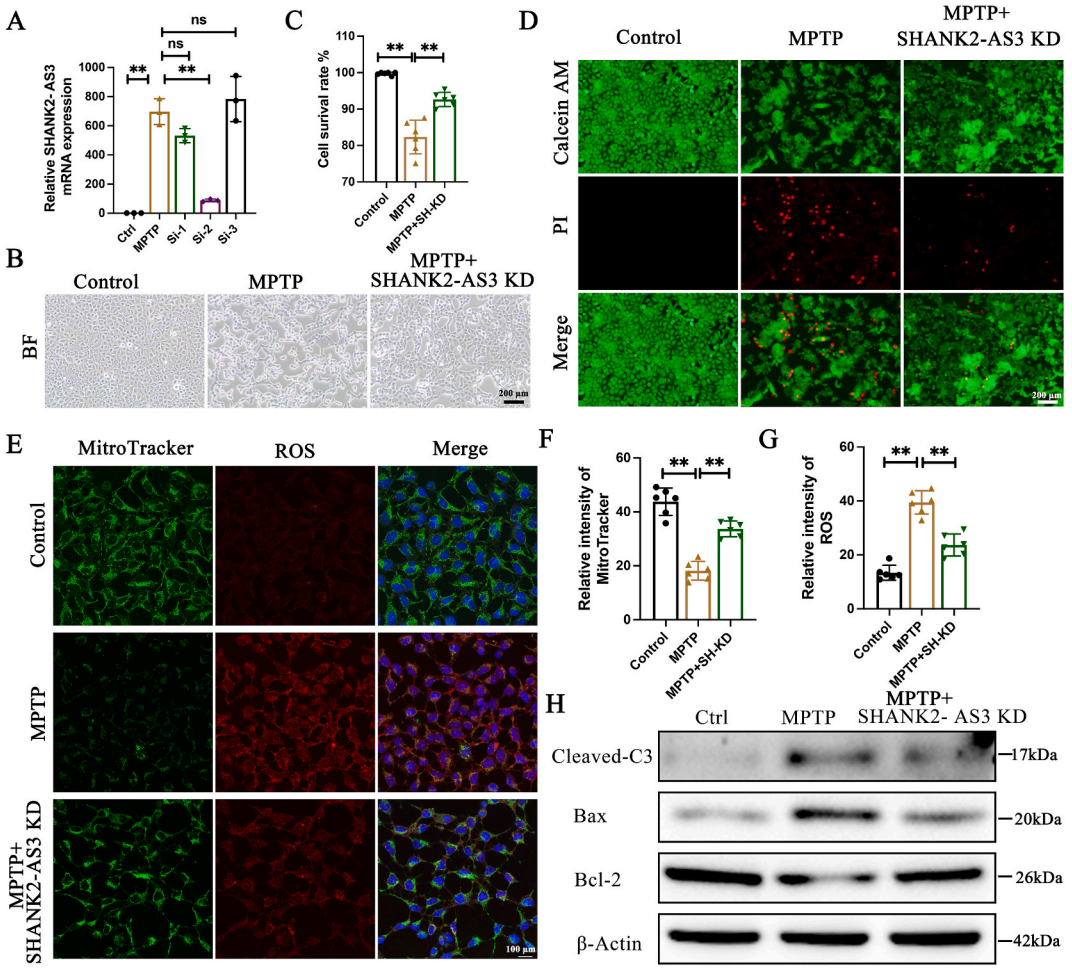

Fig. 3. Knockdown of SHANK2-AS3 Reduces Apoptosis in MPTP-Treated SH-SY5Y Cells. (A) The expression of SHANK2-AS3 was assessed in various RNAi lentivirus-infected groups within the MPTP-induced cell model. (B) Morphological comparison of SH-SY5Y cells in control, MPTP-induced, and MPTP-induced conditions combined with SHANK2-AS3 knockdown. (C–D) Quantitative analysis of neuronal cell death and Calcein-AM/PI staining in control, MPTP-induced, and MPTP-induced combined with SHANK2-AS3 knockdown conditions. (E) Assessment of mitochondrial activity and ROS accumulation in control, MPTP-induced, and MPTP-induced combined with SHANK2-AS3 knockdown groups. (F–G) Statistical analysis of the relative intensity of MitroTracker and ROS in E, respectively. (H) Western blot analysis showing the expression levels of Cleaved-Caspase3, Bax, and Bcl-2 in the different experimental conditions. Data represented as mean ± SD; $^{**}p < 0.01$; ns, no significance.

using lentiviral-mediated delivery of SHANK2-AS3-specific short hairpin RNA (shRNA). MPTP treatment significantly upregulated SHANK2-AS3 expression in SH-SY5Y cells, whereas SHANK2-AS3-shRNA2 effectively reduced this upregulation (Fig. 3A). Therefore, SHANK2-AS3-shRNA2 was utilized to deplete SHANK2-AS3 expression in subsequent experiments. Microscopic analysis revealed that SHANK2-AS3 knockdown markedly improved the morphology of MPTP-treated SH-SY5Y cells (Fig. 3B). Additionally, SHANK2-AS3 knockdown significantly mitigated MPTP-induced cell death (Fig. 3C–D), reduced reactive oxygen species (ROS) accumulation, and restored mitochondrial function, which was impaired by MPTP treatment (Fig. 3E–G). Western blot analysis further demonstrated that SHANK2-AS3 deletion decreased the expression of apoptotic markers such as cleaved Caspase-3 and Bax, while the expression of the anti-apoptotic protein Bcl-2 was significantly elevated in SHANK2-AS3 knockdown cells compared to MPTP-treated cells (Fig. 3H). These findings indicate that SHANK2-AS3 depletion attenuates MPTP-induced apoptosis in neuronal cells, suggesting a protective role against PD-related neurotoxicity.

3.4. *SHANK2-AS3 overexpression induces apoptosis in neuronal cells*

To investigate the potential role of SHANK2-AS3 in neuronal damage, we overexpressed SHANK2-AS3 in SH-SY5Y cells using lentiviral transduction. qPCR analysis confirmed a significant upregulation of SHANK2-AS3 in the SHANK2-AS3-overexpressing SH-SY5Y cells (Fig. 4A). Similar to the effects of MPTP treatment, SHANK2-AS3 overexpression resulted in elevated levels of pro-apoptotic markers Cleaved-caspase3 and Bax, while the anti-apoptotic protein Bcl-2 was significantly downregulated (Fig. 4B). Moreover, SHANK2-AS3 overexpression led to a marked increase in reactive oxygen species (ROS) accumulation and a reduction in mitochondrial function in SH-SY5Y cells (Fig. 4C–E). These results suggest that SHANK2-AS3 overexpression promotes apoptosis in SH-SY5Y cells, further supporting its role in neuronal damage and implicating SHANK2-AS3 as a potential contributor to Parkinson's disease

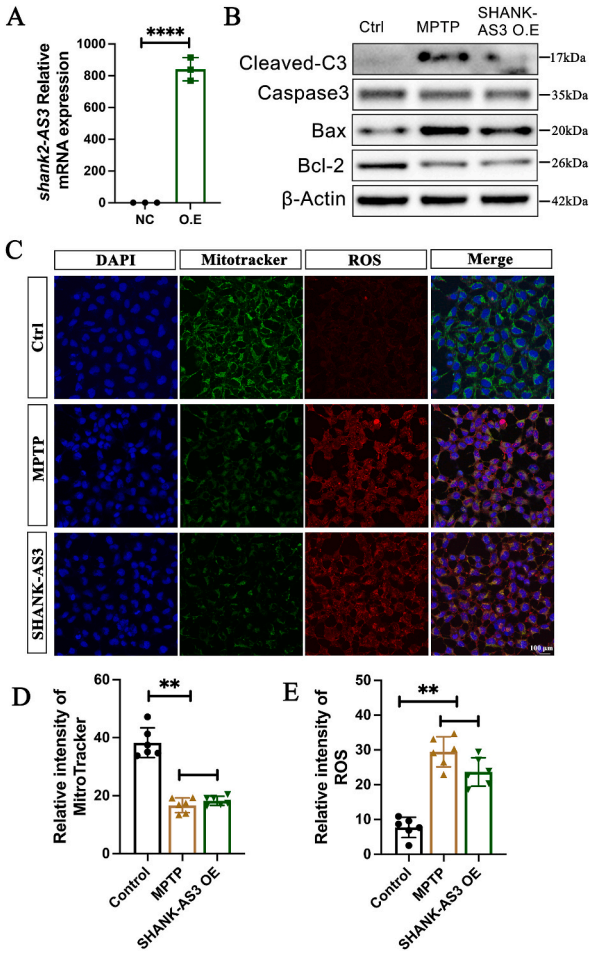

Fig. 4. SHANK2-AS3 overexpression induced the apoptosis of SH-SY5Y. (A) The expression of SHANK2-AS3 in NC and SHANK2-AS3 overexpression lentivirus infection group. (B) Western blot analysis showing the expression levels of Cleaved-Caspase3, Caspase3, Bax, and Bcl-2 in the control, MPTP-induced cells and SHANK2-AS3 overexpression groups, respectively. (C) Detection of mitochondrial activity and ROS accumulation in control, MPTP-induced, and SHANK2-AS3 overexpression groups. Statistical analysis of the relative intensity of Mitrotracker (D) and ROS (E) of C. Data represented as mean ± SD; $^{**}p < 0.01$, $^{****}p < 0.0001$.

pathogenesis.

3.5. RNA-seq profiling reveals enriched pathways associated with SHANK2-AS3 overexpression in neuronal cells

To further explore the mechanisms underlying the pro-apoptotic effects of SHANK2-AS3, RNA sequencing (RNA-seq) was performed on SH-SY5Y cells overexpressing SHANK2-AS3 and control cells. The analysis identified 156 differentially expressed mRNAs ($p < 0.05$, $|\log2FC| > 2$), consisting of 100 upregulated and 56 downregulated transcripts (Fig. 5A and B). Gene Ontology (GO) analysis revealed that SHANK2-AS3 overexpression impacts a wide range of biological, cellular, and molecular processes (Fig. 5C).

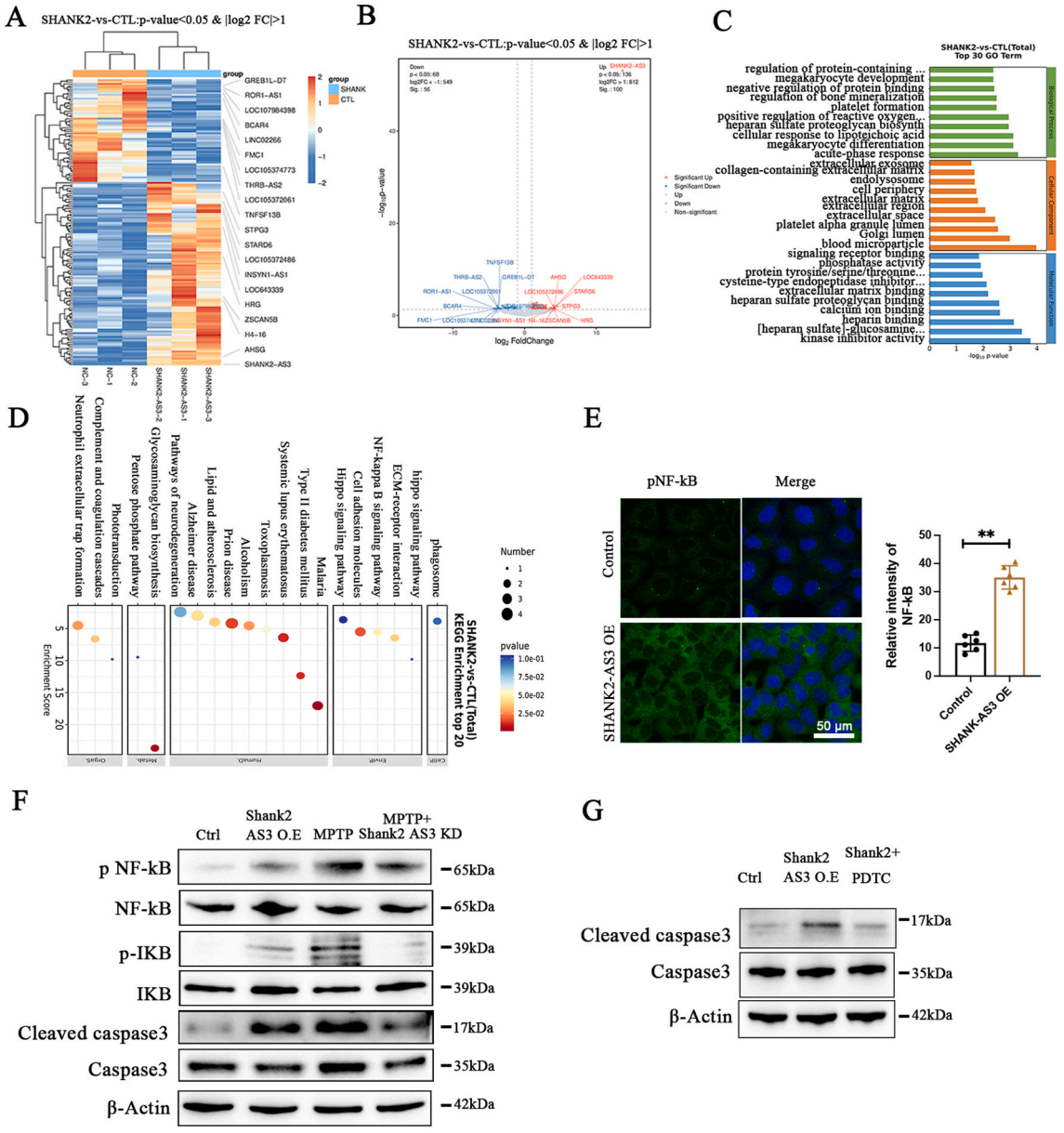

Fig. 5. RNA-Seq profiling of SHANK2-AS3 overexpression in SH-SY5Y. (A) Hierarchical clustering of differentially expressed RNA in SHANK2-AS3 overexpression group compared with control group. (B) Volcano plot illustrating differentially expressed genes in SHANK2-AS3 overexpression group compared with control group. (C) GO analysis of biological process, cellular components, and molecular function in differently expressed genes in SHANK2-AS3 overexpression group compared with control group. (D) The top30 enriched KEGG pathway in SHANK2-AS3 overexpressed SH-SY5Y. (E) Immunostaining of pNF-kB in SHANK2-AS3 overexpression group compared with control group. (F) Western blot analysis of the protein level of pNF-kB, NF-kB, p-IKB, IKB, Cleaved-caspase3, Caspase3 in control, SHANK2-AS3 overexpression, MPTP-induced, and SHANK2-AS3 knockdown in MPTP-induced SH-SY5Y. (G) Western blot analysis of the protein level of Cleaved-caspase3 and Caspase3 in control, SHANK2-AS3 overexpression, and SHANK2-AS3 treatment with PDTC in SH-SY5Y cells. Data represented as mean ± SD; $^{**}p < 0.01$.

Additionally, KEGG pathway analysis indicated that the NF-κB signaling pathway could potentially mediate the regulatory effects of SHANK2-AS3 (Fig. 5D). Immunostaining confirmed a substantial increase in pNF-κB expression in SHANK2-AS3-overexpressing SH-SY5Y cells compared to controls (Fig. 5E). Furthermore, Western blot analysis showed that both pNF-κB and p-IKB were significantly activated in SHANK2-AS3-overexpressing cells, as well as in MPTP-treated SH-SY5Y cells. In contrast, SHANK2-AS3 knockdown in MPTP-treated SH-SY5Y cells led to a downregulation of pNF-κB and p-IKB (Fig. 5F). To further investigate whether NF-κB signaling is involved in SHANK2-AS3-mediated apoptosis, the NF-κB inhibitor PDTC was applied to SH-SY5Y cells overexpressing SHANK2-AS3. The results demonstrated that PDTC effectively reversed the elevated levels of cleaved caspase-3 protein induced by SHANK2-AS3 overexpression in SH-SY5Y cells (Fig. 5G). The above results demonstrate that NF-kB participate in the SHANK2-AS3 induced cell apoptosis in neuronal cell.

3.6. CeRNA network of SHANK2-AS3

Growing evidence indicates that lncRNAs can function as competitive endogenous RNAs (ceRNAs) by directly interacting with microRNAs. To further investigate the role of SHANK2-AS3 in this context, a SHANK2-AS3-miRNA-mRNA ceRNA network was constructed using the miRcode database. As illustrated in Fig. 6, SHANK2-AS3 is predicted to bind directly to hsa-miR-146b-5p and hsa-miR-4735-3p. Moreover, hsa-miR-146b-5p is predicted to target multiple genes, including AGO1, ARL8a, ATP13A3, AVL9, BCL7B, and BRWD1, while hsa-miR-4735-3p is predicted to target GIGYF1, RAB5C, VMA21, BDH1, and CREBL2. This network suggests a complex regulatory mechanism through which SHANK2-AS3 may influence gene expression in Parkinson's disease.

4. Discussion

Parkinson's disease is the second most common neurodegenerative disorder globally. Despite its prevalence, the precise etiology of PD remains unclear, and effective therapeutic options are still lacking. Recent studies suggest that dysregulated long non-coding RNAs (lncRNAs) may play a critical role in the pathogenesis of PD. In this study, we identified SHANK2-AS3 as a differentially expressed lncRNA in PD patients, indicating its potential involvement in the disease mechanisms. Elevated levels of SHANK2-AS3 in peripheral blood of PD patients, compared to controls, suggest a potential association with the disease. The confirmation of SHANK2-AS3 upregulation in an independent patient cohort further supports its potential as a PD biomarker. Functional analysis revealed a significant increase in SHANK2-AS3 expression in MPTP-induced SH-SY5Y cells. Importantly, SHANK2-AS3 knockdown mitigated MPTP-induced neuronal apoptosis, while its overexpression exacerbated apoptosis in SH-SY5Y cells. These findings suggest that SHANK2-AS3 could be a promising therapeutic target for reducing neuronal damage in PD.

SHANK2-AS3 is an antisense RNA that co-localizes with SHANK2, which is crucial for proper synaptic development and function [20]. SHANK2 is expressed in the cortex, thalamus, dentate gyrus, and hippocampus [21]. Mutations in SHANK2 have been associated with autism spectrum disorder (ASD) [22,23]. It has been reported that SHANK2-AS3 participates in ASD by inhibiting SHANK2 expression through direct binding [24]. However, the involvement of SHANK2-AS3 in PD remains unexplored. In our study, we observed an upregulation of SHANK2-AS3 in the peripheral blood of PD patients through bioinformatics analysis using the GEO dataset. This finding was further validated by confirming that SHANK2-AS3 expression was significantly elevated in PD patients. Notably, the area under the curve (AUC) for SHANK2-AS3 was 0.78, suggesting its potential as a biomarker for PD.

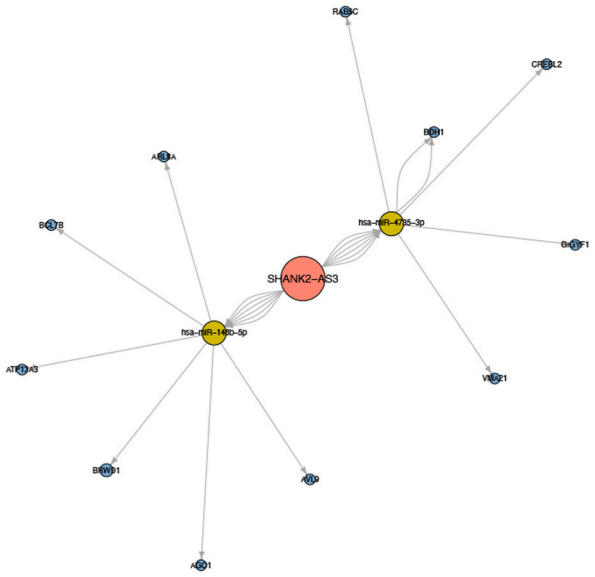

Fig. 6. CeRNA network of SHANK2-AS3. The potential interaction of SHANK2-AS3 with miRNA and mRNA.

Cell apoptosis is a crucial factor in the pathogenesis of PD. Various factors, such as oxidative stress, endoplasmic reticulum (ER) stress, DNA damage, and cytosolic Ca2+ overload, can trigger intrinsic apoptosis in PD [7]. Mitochondrial outer membrane permeabilization (MOMP) is a key event in intrinsic apoptosis, regulated by the balance between pro-apoptotic and anti-apoptotic members of the Bcl-2 family [25]. Specifically, the proteins BAX and BAK are critical for the formation of MOMP and play an essential role in apoptosis. Previous studies have shown that in MPTP-induced SH-SY5Y cells, Bcl-2 expression is decreased while Bax expression is increased [26,27]. Our study also observed that MPTP-induced neuronal apoptosis is associated with the regulation of Bcl-2 and Bax expression. Furthermore, SHANK2-AS3 was significantly upregulated in MPTP-treated SH-SY5Y cells. Knockdown of SHANK2-AS3 substantially reduced MPTP-induced cell death, decreased ROS generation, and improved mitochondrial function in SH-SY5Y cells. Conversely, overexpression of SHANK2-AS3 led to increased cell apoptosis, enhanced ROS accumulation, and diminished mitochondrial activity. Recent studies have shown that ferroptosis plays a significant role in PD, particularly in the degenerative changes of dopaminergic neurons, where abnormal iron metabolism is closely linked to oxidative stress [28]. The mechanism of ferroptosis is considered a key factor contributing to neuronal damage, but whether SHANK2-AS3 plays a regulatory role in this process remains unclear. Our study utilized a PD cell model involving SH-SY5Y cells treated with MPTP to investigate this issue. Future research should focus on validating the role of SHANK2-AS3 in neuronal death within animal models and explore its potential as a therapeutic target for Parkinson's disease.

RNA-seq analysis revealed significant enrichment of the NF-κB signaling pathway in SHANK2-AS3-overexpressing SH-SY5Y cells. The NF-κB pathway is known to play a dual role in apoptosis, acting as both a pro-survival and pro-apoptotic regulator depending on the cellular context [29]. In PD, dysregulation of NF-κB signaling has been implicated in neurodegeneration and disease progression. Specifically, activation of NF-κB has been shown to promote neuronal apoptosis in PD patients [30]. Our study found a marked upregulation of pNF-κB and p-IKKB in SHANK2-AS3-overexpressing and MPTP-induced SH-SY5Y cells, whereas these levels were reduced in the SHANK2-AS3 knockdown group. Furthermore, in SHANK2-AS3-overexpressing SH-SY5Y cells, treatment with an NF-κB inhibitor effectively diminished the expression of Cleaved-caspase3 induced by SHANK2-AS3 overexpression. However, additional research is needed to elucidate the precise mechanism by which SHANK2-AS3 regulates NF-κB signaling.

The ceRNA network analysis identified potential interactions between SHANK2-AS3, microRNAs (miRNAs), and target mRNAs. We found that the hsa-miR-146b-5p and hsa-miR-4735-3p might be the direct target of the SHANK2-AS3 and participated in the cell apoptosis of PD. This ceRNA crosstalk may contribute to the dysregulation of key genes involved in PD pathology. Further exploration of the SHANK2-AS3-miRNA-mRNA network could provide insights into the molecular mechanisms underlying PD development and progression.

Overall, the study reveals the potential role of SHANK2-AS3 in the pathogenesis of PD, highlighting its potential as a diagnostic biomarker and therapeutic target. We found that SHANK2-AS3 is significantly upregulated in peripheral blood of PD patients and shows a similar increase in the MPTP-induced SH-SY5Y cell model. This suggests that SHANK2-AS3 may be associated with the pathological processes of PD. Functional analysis indicates that overexpression of SHANK2-AS3 exacerbates neuronal apoptosis, while its knockdown effectively alleviates MPTP-induced cell death and oxidative stress, suggesting that SHANK2-AS3 may impact PD-related neuronal damage by regulating apoptotic pathways. Additionally, we found that SHANK2-AS3 plays a role in apoptosis through the modulation of the NF-κB signaling pathway and may interact with specific miRNAs and target mRNAs via the ceRNA network. These findings provide new insights into the mechanisms underlying the role of SHANK2-AS3 in PD and lay a solid foundation for future research, particularly in developing targeted therapeutic strategies against SHANK2-AS3.

Funding

This work was supported by the Shanghai Municipal Health Commission under Grant no. 20214Y0432, Changning district Health Commission under Grant no. 20194Y005, Changning district Health Commission under Grant no. CNJH08, and 20214Y002, Changning District Science and Technology Commission Grant no. CNKW2020Y04.

Data availability

The datasets analyzed in this study are accessible from the corresponding author upon reasonable request.

Ethics approval and consent to participate

This study received approval from the Medical Ethics Committee of Shanghai Tongren Hospital (approval number: 2018-030-01).

Disclosure statement

The authors report no conflict of interest.

CRediT authorship contribution statement

Qiong Huang: Validation, Funding acquisition, Data curation, Conceptualization. **Dani Qin:** Validation. **Chunyan Chen:** Methodology, Funding acquisition, Data curation, Conceptualization. **Yu Kang:** Supervision, Methodology. **Haocong Chen:** Validation, Methodology. **Min Xu:** Visualization, Validation, Conceptualization. **Rao Fu:** Writing – original draft, Funding acquisition,

Conceptualization. **Xiaohua Dong:** Writing – review & editing, Writing – original draft, Project administration, Conceptualization.

Declaration of competing interest

The authors declare that they have no known competing financial interests or personal relationships that could have appeared to influence the work reported in this paper.

Appendix A. Supplementary data

Supplementary data to this article can be found online at https://doi.org/10.1016/j.heliyon.2024.e38822.

References

[1] L.V. Kalia, A.E. Lang, Parkinson's disease, Lancet 386 (2015) 896–912.
[2] Y. Ben-Shlomo, S. Darweesh, J. Llibre-Guerra, C. Marras, M. San Luciano, C. Tanner, The epidemiology of Parkinson's disease, Lancet 403 (2024) 283–292.
[3] J. Jankovic, Parkinson's disease: clinical features and diagnosis, J. Neurol. Neurosurg. Psychiatry 79 (2008) 368–376.
[4] A.H.V. Schapira, K.R. Chaudhuri, P. Jenner, Non-motor features of Parkinson disease, Nat. Rev. Neurosci. 18 (2017) 435–450.
[5] A. Ascherio, M.A. Schwarzschild, The epidemiology of Parkinson's disease: risk factors and prevention, Lancet Neurol. 15 (2016) 1257–1272.
[6] X. Dong-Chen, C. Yong, X. Yang, S. Chen-Yu, P. Li-Hua, Signaling pathways in Parkinson's disease: molecular mechanisms and therapeutic interventions, Signal Transduct Target Ther 8 (2023) 73.
[7] P.A. Dionisio, J.D. Amaral, C.M.P. Rodrigues, Oxidative stress and regulated cell death in Parkinson's disease, Ageing Res. Rev. 67 (2021) 101263.
[8] S.R. Subramaniam, M.F. Chesselet, Mitochondrial dysfunction and oxidative stress in Parkinson's disease, Prog Neurobiol 106–107 (2013) 17–32.
[9] M.J. Morgan, Z.G. Liu, Crosstalk of reactive oxygen species and NF-kappaB signaling, Cell Res. 21 (2011) 103–115.
[10] L. Galluzzi, I. Vitale, S.A. Aaronson, J.M. Abrams, D. Adam, P. Agostinis, E.S. Alnemri, L. Altucci, I. Amelio, D.W. Andrews, M. Annicchiarico-Petruzzelli, A. V. Antonov, E. Arama, E.H. Baehrecke, N.A. Barlev, N.G. Bazan, F. Bernassola, M.J.M. Bertrand, K. Bianchi, M.V. Blagosklonny, K. Blomgren, C. Borner, P. Boya, C. Brenner, M. Campanella, E. Candi, D. Carmona-Gutierrez, F. Cecconi, F.K. Chan, N.S. Chandel, E.H. Cheng, J.E. Chipuk, J.A. Cidlowski, A. Ciechanover, G. M. Cohen, M. Conrad, J.R. Cubillos-Ruiz, P.E. Czabotar, V. D'Angiolella, T.M. Dawson, V.L. Dawson, V. De Laurenzi, R. De Maria, K.M. Debatin, R. J. DeBerardinis, M. Deshmukh, N. Di Daniele, F. Di Virgilio, V.M. Dixit, S.J. Dixon, C.S. Duckett, B.D. Dynlacht, W.S. El-Deiry, J.W. Elrod, G.M. Fimia, S. Fulda, A.J. Garcia-Saez, A.D. Garg, C. Garrido, E. Gavathiotis, P. Golstein, E. Gottlieb, D.R. Green, L.A. Greene, H. Gronemeyer, A. Gross, G. Hajnoczky, J.M. Hardwick, I.S. Harris, M.O. Hengartner, C. Hetz, H. Ichijo, M. Jaattela, B. Joseph, P.J. Jost, P.P. Juin, W.J. Kaiser, M. Karin, T. Kaufmann, O. Kepp, A. Kimchi, R.N. Kitsis, D. J. Klionsky, R.A. Knight, S. Kumar, S.W. Lee, J.J. Lemasters, B. Levine, A. Linkermann, S.A. Lipton, R.A. Lockshin, C. Lopez-Otin, S.W. Lowe, T. Luedde, E. Lugli, M. MacFarlane, F. Madeo, M. Malewicz, W. Malorni, G. Manic, J.C. Marine, S.J. Martin, J.C. Martinou, J.P. Medema, P. Mehlen, P. Meier, S. Melino, E.A. Miao, J.D. Molkentin, U.M. Moll, C. Munoz-Pinedo, S. Nagata, G. Nunez, A. Oberst, M. Oren, M. Overholtzer, M. Pagano, T. Panaretakis, M. Pasparakis, J. M. Penninger, D.M. Pereira, S. Pervaiz, M.E. Peter, M. Piacentini, P. Pinton, J.H.M. Prehn, H. Puthalakath, G.A. Rabinovich, M. Rehm, R. Rizzuto, C.M. P. Rodrigues, D.C. Rubinsztein, T. Rudel, K.M. Ryan, E. Sayan, L. Scorrano, F. Shao, Y. Shi, J. Silke, H.U. Simon, A. Sistigu, B.R. Stockwell, A. Strasser, G. Szabadkai, S.W.G. Tait, D. Tang, N. Tavernarakis, A. Thorburn, Y. Tsujimoto, B. Turk, T. Vanden Berghe, P. Vandenabeele, M.G. Vander Heiden, A. Villunger, H.W. Virgin, K.H. Vousden, D. Vucic, E.F. Wagner, H. Walczak, D. Wallach, Y. Wang, J.A. Wells, W. Wood, J. Yuan, Z. Zakeri, B. Zhivotovsky, L. Zitvogel, G. Melino, G. Kroemer, Molecular mechanisms of cell death: recommendations of the nomenclature committee on cell death 2018, Cell Death Differ. 25 (2018) 486–541.
[11] T.R. Mercer, M.E. Dinger, S.M. Sunkin, M.F. Mehler, J.S. Mattick, Specific expression of long noncoding RNAs in the mouse brain, Proc Natl Acad Sci U S A 105 (2008) 716–721.
[12] P. Wan, W. Su, Y. Zhuo, The role of long noncoding RNAs in neurodegenerative diseases, Mol. Neurobiol. 54 (2017) 2012–2021.
[13] Q. Lin, S. Hou, Y. Dai, N. Jiang, Y. Lin, LncRNA HOTAIR targets miR-126-5p to promote the progression of Parkinson's disease through RAB3IP, Biol. Chem. 400 (2019) 1217–1228.
[14] F.A. Boros, L. Vecsei, P. Klivenyi, NEAT1 on the field of Parkinson's disease: offense, defense, or a player on the bench? J. Parkinsons Dis. 11 (2021) 123–138.
[15] K. Li, Z. Wang, lncRNA NEAT1: key player in neurodegenerative diseases, Ageing Res. Rev. 86 (2023) 101878.
[16] E. Mutez, L. Larvor, F. Lepretre, V. Mouroux, D. Hamalek, J.P. Kerckaert, J. Perez-Tur, N. Waucquier, C. Vanbesien-Mailliot, A. Duflot, D. Devos, L. Defebvre, A. Kreisler, B. Frigard, A. Destee, M.C. Chartier-Harlin, Transcriptional profile of Parkinson blood mononuclear cells with LRRK2 mutation, Neurobiol. Aging 32 (2011) 1839–1848.
[17] R.B. Postuma, D. Berg, M. Stern, W. Poewe, C.W. Olanow, W. Oertel, J. Obeso, K. Marek, I. Litvan, A.E. Lang, G. Halliday, C.G. Goetz, T. Gasser, B. Dubois, P. Chan, B.R. Bloem, C.H. Adler, G. Deuschl, MDS clinical diagnostic criteria for Parkinson's disease, Mov. Disord. 30 (2015) 1591–1601.
[18] J. Zhao, M. Le, J. Li, Q. Huang, H. Chen, W. Zhang, H. Mao, Q. Sun, A. Li, Y. Zhao, L. Yu, M. Yi, J. Wang, X. Li, G. Zhang, J. Ma, X. Dong, LINC00938 alleviates hypoxia ischemia encephalopathy induced neonatal brain injury by regulating oxidative stress and inhibiting JNK/p38 MAPK signaling pathway, Exp. Neurol. 367 (2023) 114449.
[19] H. Chen, Y. Wusiman, J. Zhao, W. Zhang, W. Liu, S. Wang, G. Qian, G. Zhang, M. Le, X. Dong, Metabolomics analysis revealed the neuroprotective role of 2-phosphoglyceric acid in hypoxic-ischemic brain damage through GPX4/ACSL4 axis regulation, Eur. J. Pharmacol. 971 (2024) 176539.
[20] M. Sheng, C.C. Hoogenraad, The postsynaptic architecture of excitatory synapses: a more quantitative view, Annu. Rev. Biochem. 76 (2007) 823–847.
[21] P. Monteiro, G. Feng, SHANK proteins: roles at the synapse and in autism spectrum disorder, Nat. Rev. Neurosci. 18 (2017) 147–157.
[22] K. Zaslavsky, W.B. Zhang, F.P. McCready, D.C. Rodrigues, E. Deneault, C. Loo, M. Zhao, P.J. Ross, J. El Hajjar, A. Romm, T. Thompson, A. Piekna, W. Wei, Z. Wang, S. Khattak, M. Mufteev, P. Pasceri, S.W. Scherer, M.W. Salter, J. Ellis, SHANK2 mutations associated with autism spectrum disorder cause hyperconnectivity of human neurons, Nat. Neurosci. 22 (2019) 556–564.
[23] Y. Zhou, T. Kaiser, P. Monteiro, X. Zhang, M.S. Van der Goes, D. Wang, B. Barak, M. Zeng, C. Li, C. Lu, M. Wells, A. Amaya, S. Nguyen, M. Lewis, N. Sanjana, Y. Zhou, M. Zhang, F. Zhang, Z. Fu, G. Feng, Mice with Shank3 mutations associated with ASD and schizophrenia display both shared and distinct defects, Neuron 89 (2016) 147–162.
[24] T. Luo, P. Liu, X.Y. Wang, L.Z. Li, L.P. Zhao, J. Huang, Y.M. Li, J.L. Ou, X.Q. Peng, Effect of the autism-associated lncRNA Shank2-AS on architecture and growth of neurons, J. Cell. Biochem. 120 (2019) 1754–1762.
[25] S.W. Tait, D.R. Green, Mitochondria and cell death: outer membrane permeabilization and beyond, Nat. Rev. Mol. Cell Biol. 11 (2010) 621–632.
[26] S. Han, M.H. Seo, S. Lim, S. Yeo, Decrease in ITGA7 levels is associated with an increase in alpha-synuclein levels in an MPTP-induced Parkinson's disease mouse model and SH-SY5Y cells, Int. J. Mol. Sci. 22 (2021).
[27] L. Rani, B. Ghosh, M.H. Ahmad, A.C. Mondal, Evaluation of potential neuroprotective effects of vanillin against MPP(+)/MPTP-Induced dysregulation of dopaminergic regulatory mechanisms in SH-SY5Y cells and a mouse model of Parkinson's disease, Mol. Neurobiol. 60 (2023) 4693–4715.

[28] X.S. Ding, L. Gao, Z. Han, S. Eleuteri, W. Shi, Y. Shen, Z.Y. Song, M. Su, Q. Yang, Y. Qu, D.K. Simon, X.L. Wang, B. Wang, Ferroptosis in Parkinson's disease: molecular mechanisms and therapeutic potential, Ageing Res. Rev. 91 (2023) 102077.
[29] G.E. Sonenshein, Rel/NF-kappa B transcription factors and the control of apoptosis, Semin. Cancer Biol. 8 (1997) 113–119.
[30] M. Alrouji, H.M. Al-Kuraishy, A.I. Al-Gareeb, A. Alexiou, M. Papadakis, M.S. Jabir, H.M. Saad, G.E. Batiha, NF-kappaB/NLRP3 inflammasome axis and risk of Parkinson's disease in Type 2 diabetes mellitus: a narrative review and new perspective, J. Cell Mol. Med. 27 (2023) 1775–1789.